The effect of immobilized catalyst structure on the degradation of chemical and biological contaminants in simulated solar photocatalytic water purification

Stephanie Loeb, Susan A. Andrews and Ron Hofmann

ABSTRACT

The performance of different configurations of titanium dioxide-coated foam supports as photocatalysts in an enhanced solar disinfection system for drinking water treatment was evaluated, using the reduction of methylene blue, 1-4-dioxane, and *Escherichia coli* as performance indicators. Reactors with immobilized catalysts were able to match or surpass the performance of a suspension configuration due to effective mass transport and association between the analyte and the foam. Performance was related to the pore size of the foam, with the ideal pore size varying between target contaminants.

Key words | 1,4-dioxane, advanced oxidation, *Escherichia coli*, immobilization, photocatalysis

Stephanie Loeb (corresponding author)
Susan A. Andrews
Ron Hofmann
Department of Civil Engineering,
University of Toronto,
35. St George St., Toronto, ON,
Canada,
M5S 1A4
E-mail: *stephanie.loeb@mail.utoronto.ca*

INTRODUCTION

Solar disinfection (SODIS) is a well-known cost-effective mechanism for the inactivation of disease-causing organisms in water. The SODIS process involves the exposure of water in polyethylene terephthalate bottles to direct solar radiation for a minimum of 6 hours, after which the pathogen load is decreased and the quality of the water substantially improved. The inactivation caused by SODIS treatment is understood to involve several modes of action resulting from the absorption of short wavelength UV radiation and long wavelength infrared thermal radiation (Meierhofer & Wegelin, 2002; Blanco *et al.* 2009; Byrne *et al.* 2011). The integration of solar photocatalytic advanced oxidation into the SODIS method has been proposed as a robust approach for improving the microbial and chemical quality of the treated water (Lonnen *et al.* 2005; Shannon *et al.* 2008; Blanco *et al.* 2009; Byrne *et al.* 2011). The goal of this integration is to develop a small and inexpensive point-of-use photoreactor.

One aspect of photoreactor design is the photocatalyst configuration, which refers to the shape or form of the catalyst within the reactor. Variations include different sized particulate suspensions, immobilized thin films, and three-dimensional support structures that are coated by the photocatalytic material (Kisch & Macyk, 2002; Guiang *et al.* 2008; Li *et al.* 2008; Akhavan *et al.* 2009; Han *et al.* 2011; Zhang, 2012; Zhang *et al.* 2012). Traditionally, suspended systems have been common and are an efficient configuration, but the catalyst must be removed before consumption requiring the application of a chemical treatment or fine filter which may not be cheaply available and complicates the purification process (Gumy *et al.* 2006; Plantard *et al.* 2011). Therefore, immobilization of the photocatalyst remains an attractive alternative, particularly for small scale point-of-use applications.

One way to immobilize the photocatalytic material is to use a foam support. Foam is considered attractive because it has high porosity, high surface area, low density, and high permeability, all of which promote high efficiency reactions (Antoniou *et al.* 2009; Plesch *et al.* 2009; Plantard *et al.* 2011). A broad comparison of catalyst configurations including a wide range of foam pore sizes, suspension and fixed film reactors has not been empirically undertaken. Furthermore, in past investigations that have been performed with probe compounds, the relationship between configuration performance and target compound has not been described,

doi: 10.2166/aqua.2015.035

particularly for biological contaminants and common environmental pollutants.

The following presents a case study in which the performance of different photocatalytic foams are compared in SODIS-like conditions. The study presented has the two-fold aim of: (i) predicting the best configuration for an immobilized catalyst in an enhanced SODIS reactor by evaluating the comparative performance of TiO_2 coated foams of varying pore size, a TiO_2 suspension and TiO_2 fixed film photocatalyst configurations; and (ii) examining the relationship between target contaminant degradation and reactor configuration. For this second aim, the degradation for each reactor configuration was evaluated for methylene blue (MB) as a probe compound, *Escherichia coli* as an indicator of biological contaminants, and 1,4-dioxane as a common environmental pollutant.

MATERIAL AND METHODS

Photocatalytic material preparation and characterization

Aluminum foams, shown in Figure 1, were purchased from ERG Materials and Aerospace. Foams had an average relative density of $7.85\% \pm 0.95\%$, which represents the mass of the foam material divided by the mass the material would be if it were a solid block of the same dimensions, as determined by the manufacturer. All foam samples were cylindrical with a height of 2 cm and a diameter of 6 cm. Four pore sizes (5, 10, 20 and 40 pores per inch (PPI)) were selected in order to cover a wide range of mesh densities, in turn, increasing the likelihood of detecting an optimum pore size. As the number of PPI increases, the mesh density of the foam increases, creating a more intricate structure with a greater surface area to volume ratio. Although foams were designed to have a relatively density between 6 and 10%, it was found that the foams with a greater number of PPI tended to weigh more by ~2 g and have relative density on the higher end of the indicated range. Fixed films were made with a flat sheet of aluminum metal cut into circular pieces with a 5 cm diameter.

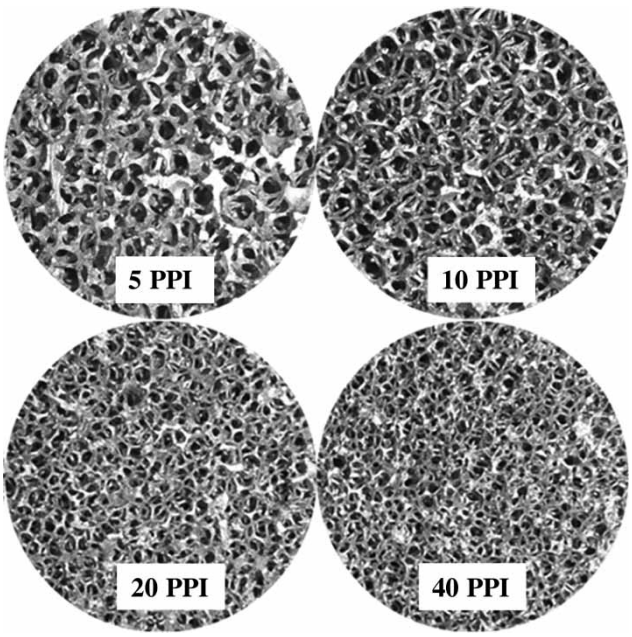

Figure 1 | Aluminum foams with 5, 10, 20 and 40 PPI.

Materials were coated by an adaptation of the dip coating method described by Plesch *et al.* (2009) using an acidified mixture of 20% (by weight) Aeroxide P-25® TiO_2 in distilled water and a heat treatment at 600 °C with a ramp rate of 2.5 °C/min.

Bench-scale solar simulator photocatalytic degradation experiments

Irradiation experiments were performed in a Photoemission Tech SS150AA solar simulator which employs a xenon short arc lamp and an AM1.5 G (Atmospheric Mass 1.5; Global) filter to deliver solar spectrum light in an illumination field of 156×156 mm. Prior to experimentation, the system was adjusted to produce light equivalent to a one sun intensity. Spatial and temporal uniformity of the light (rated at $\leq$2%) were confirmed by external calibration and verification with a photo diode and multimeter. Spatial non-uniformity was determined to be 0.84% across the *x*-axis and 1.19% across the *y*-axis, which was also the maximum non-uniformity. Temporal non-uniformity over a 4.5 hour period was determined to be 1.25%. Temperature was observed to rise steadily over the first 60 minutes, and then remain constant throughout the remainder of the time. The average ambient room temperature was 22.5 °C and the maximum temperature reached inside the reactor was 32.5 °C. During experimentation, the sides of the

reactor were covered with a dark material to prevent ambient light from hitting the samples from the side. Experiments were performed with the test samples exposed to ambient air. Samples were arranged as shown in Figure 2 with the control sample in the centre and each other sample spaced evenly around the centre. This arrangement ensures that each of the samples containing catalyst is an equal distance from the centre of the reactor. Each sample was contained in a small crystallizing dish (70 × 50 mm; Fisher Scientific), holding one foam of each indicated pore size, a coated fixed-film, powered TiO_2, and a vacant dish for the control sample. Samples were placed in the solar simulator illumination area and filled with 75 mL deionized (DI) water for dye and chemical experiments and ¼ strength Ringer's solution for *E. coli* samples. Sample pH was consistent at 6.5 ± 0.5. Each container was then dosed with a single contaminant as described below and briefly stirred to create a homogeneous mixture. The first sample was taken immediately after dosing. Suspended Aeroxide P-25® TiO_2, TiO_2 coated aluminum foams and flat aluminum fixed TiO_2 film materials were then added to the dishes.

The samples were kept in the dark for a 30 minute dark reaction before the lamp shutter was opened. For the 1,4-dioxane and MB samples one aliquot from each container was removed at 0, 5, 10, 20, 40, 80, 120 and 160 minutes. *E. coli* samples were removed at 0, 15, 30, 45, 60 and 75 minutes. Samples were not stirred continuously throughout the exposure in order to mimic SODIS reactor conditions; however, each sample was briefly stirred immediately prior to sampling to achieve an accurate sample with uniform distribution of contaminant prior to measurement. Individual foams were not re-used because the coating method was not optimized for these exploratory tests nor were the foams confirmed to be effective over longer periods of time.

Contaminant dosing and detection

One of the principal aims of this study was to investigate the relationship between photoreactor configuration with different types of contaminants to further describe the dependence of comparative reactor efficiency on the choice of test compound. We selected one representative

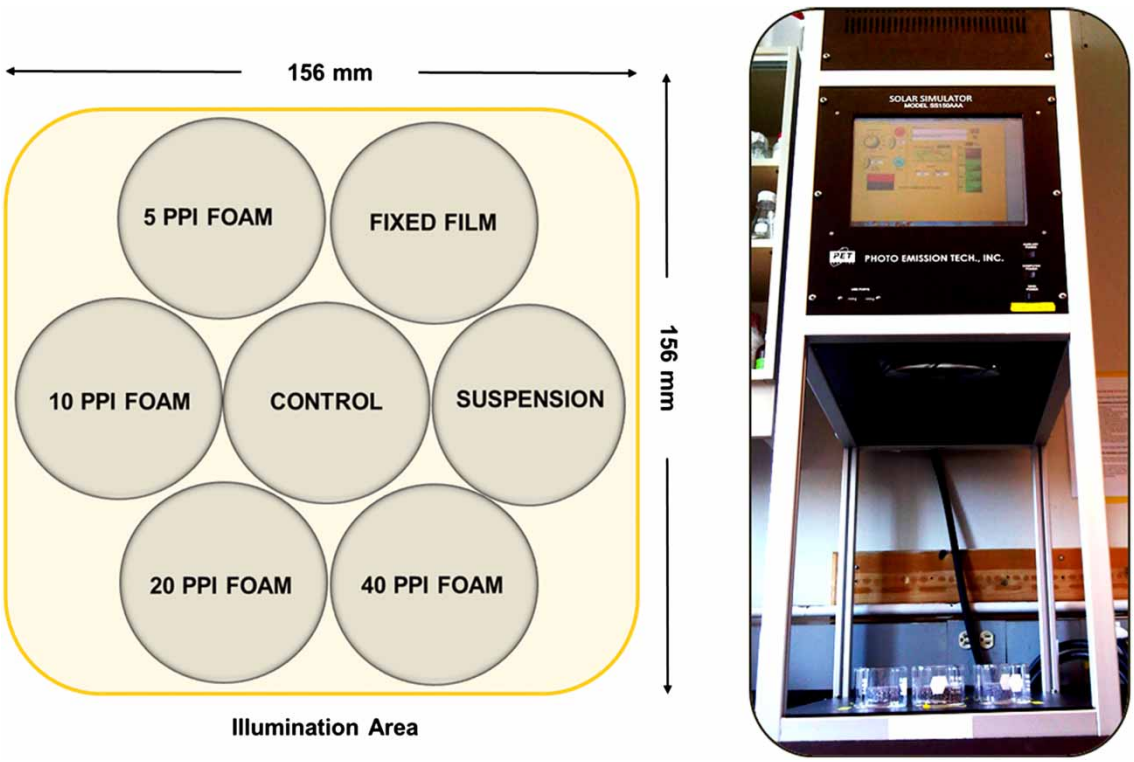

Figure 2 | Left – reactors arranged in solar simulator during treatment; right – photoemission Tech SS150AA solar simulator.

compound from three categories: a probe compound to indirectly monitor hydroxyl radical (·OH) formation, a chemical pollutant, and a biological contaminant/pathogen. The probe compound selected was MB, one of the most commonly applied organic dyes, because of its ease of detection and extensive use in past literature (Wang & Ku, 2006; Natarajan *et al.* 2011; Sahoo & Gupta, 2012). Colored dyes are easily measured using spectrophotometric methods making them particularly good candidates for an initial investigation. 1,4-dioxane was chosen as the chemical pollutant because it is a recalcitrant organic that is not known to break down or be removed significantly by conventional methods. The pathogen selected was *E. coli*, a common contaminant in drinking water globally and a good indicator organism for predicting the presence of other micro-organisms. There is also a vast wealth of research that has been conducted on the treatment of *E. coli* using a variety of treatment methods (Acra *et al.* 1990; Galalgorchev, 1992; Cho *et al.* 2004; Lonnen *et al.* 2005).

MB samples (Fischer Scientific) were prepared by dissolving 200 mg/L of the dye into DI water. Two mL of this solution per liter of water sample was added to the photoreactor immediately prior to experimentation to achieve a starting concentration of 4 mg/L. Concentration was determined using a diode array UV-vis spectrophotometer at 663 nm. Suspension samples were spun down in a centrifuge before analysis to pellet and remove the TiO_2.

Samples were dosed with 100 ppm 1,4-dioxane immediately prior to experimentation to achieve a concentration of 1 ppm. Suspension samples were filtered through a 0.45 μm Acrodisc syringe filter before analysis. A fixed concentration of an isoptic labeled surrogate internal calibration standard (1,4-dioxane-d_8; Sigma Aldrich) was added to each aliquot after sampling. Dioxane and its surrogate standard in the water samples were extracted using liquid–liquid extraction with a solution of hexane-dichloromethane (80:20, v/v) followed by concentration through solid phase extraction with a C_{18} SPE cartridge and elution with acetonitrile (Luck & Hofmann, 2006). The eluted sample was collected in 2 mL amber vials and run on a gas chromatograph with a DB1701 column, showing a dioxane retention time of 8–9 minutes. The concentration of 1,4-dioxane was determined through correlation with standards and by relating the mass spectrometer response of 1,4-dioxane's quantification ion (m/z 88) to the response of the 1,4-dioxane-d_8's quantification ion (m/z 96).

Bacterial preparation and enumeration were performed following ATCC guidelines and standard aseptic practices. A lyophilized *E. coli* stock culture (ATCC® 23631; Cedarlane Laboratories) was revived in LB broth (Sigma-Aldrich), grown into the logarithmic phase and used to prepare glycerol stocks. Stocks were reanimated the evening prior to experimentation and incubated overnight at 37 °C until they reached a concentration of 10^9 CFU/mL as confirmed by measuring the OD_{600}. A portion of the stationary culture at 10^9 CFU/mL was transferred to a sterile autoclaved 50 mL centrifuge tube and spun down at 3,000 rpm for 10 minutes. The growth media was removed and the pellet suspended in 25 mL of a quarter strength Ringers solution. This process was repeated twice to ensure all growth media was removed from the solution. One mL of this solution was added to 25 mL ¼ Ringers to make a stock solution for inoculation. Immediately prior to experimentation, 1 mL of the stock solution was added to 75 mL ¼ Ringers in each photoreactor configuration, resulting in a starting concentration of ~10^6 CFU/mL. At the indicated time intervals, the bacterial levels were enumerated using the following standard spread plate count method. First, 1 mL sample was taken from the culture and serially diluted with sterile phosphate buffer saline (PBS; Sigma-Aldrich) solution. One hundred μL of each dilution was pipetted into the middle of a sterile pre-poured LB agar 10 cm Petri plate (Sigma-Aldrich) and manually spread using a spin table and sterile spreader. Plates were incubated at 37 °C for 24 hours after which the colonies were counted.

RESULTS AND DISCUSSION

Characterization of photocatalytic coatings

Photocatalytic coatings of consistent thickness with relatively good adhesion were produced, although the mass of the coating varied between sample type and was likely dependent on its available surface area. For example, the finer pore size foams (20 and 40 PPI) supported a larger coating mass. None of the mass of catalyst was lost during each experiment, as verified by thoroughly rinsing the

foams after use and re-taking their mass. Table 1 shows the average mass of catalyst applied to each support and the variation between samples. Suspension samples contained 1 g TiO_2 for comparison.

Scanning electron microscope (SEM) images of the foam coating were taken using a JOEL JSM6610-Lv in secondary electron imaging (SEI) mode in order to characterize the morphology and surface topography of the coating. Images show that an effective distribution of the coating over the foam surface was achieved; however, there were different characteristics in the coating of foams with varying pore size. The large pore size samples (5 and 10 PPI) showed a coating with more cracks, which could be a result of the longer struts and greater distance between curves and bends, which can help to support the coating during heat treatment. Small cracks can be seen along the curved edge of the coating in Figure 3(a) and 3(b).

Table 1 | Mass and variation in photocatalytic TiO_2 coatings

5 PPI Foam	10 PPI Foam	20 PPI Foam	40 PPI Foam	Fixed Film
0.59 ± 0.06 g	0.62± 0.07 g	1.08± 0.06 g	1.16± 0.07 g	1.13± 0.05 g

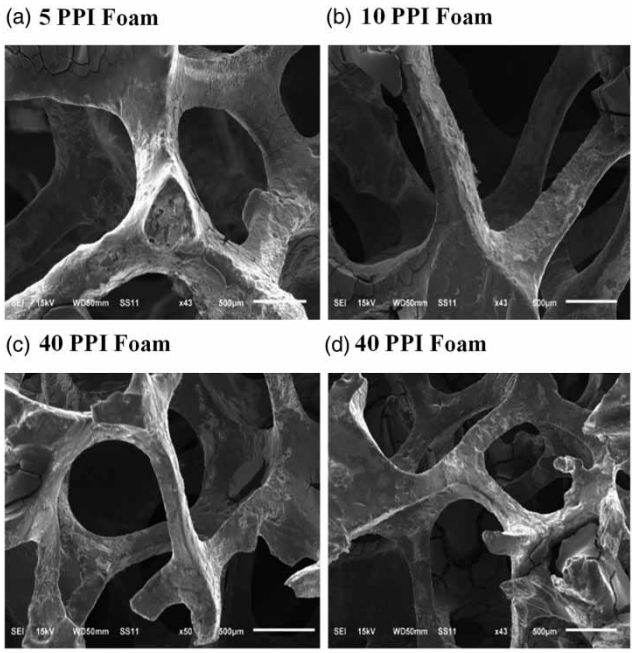

Figure 3 | SEM secondary electron images (SEI) of TiO_2 coated aluminum foams.

The 20 and 40 PPI foams showed less cracks in the coating, although more clogged pores, pores in which an agglomeration of TiO_2 accumulated, were identified. It is hypothesized that these clogs, as depicted in the bottom right hand corner of Figure 3(d), were formed by surface tension in the coating which allowed a bubble like structure to form and solidify in the pore during heat treatment. This is also supported by the partially blocked pore seen in upper right Figure 3(c), which has a structure resembling a popped bubble. It is likely that the greater portion of clogged pores also contributed to the large jump in average mass coating for the 20 and 40 PPI samples.

Contaminant degradation

MB was the first compound used to investigate the performance of each of the photoreactor configurations: suspension, foams with 5, 10, 20 and 40 PPI, and fixed films.

Prior to testing photocatalytic degradation, the photolytic removal of 4 mg/L of MB was first measured in samples containing foams without TiO_2 coating, as well as in a DI water only sample. These control experiments were performed with the aim of determining the extent of the photolytic degradation of MB to quantify the amount of light obscured by the foams. Some degradation of the MB dye is expected in the presence of simulated sunlight even without a catalyst as a result of direct photolysis by the high energy near UV wavelengths present at the far blue end of the radiation. The results of this control test showed direct photodegradation of MB varying between 24 and 42%. The least discolouration (24%) occurred in the samples containing the smallest pore size (40 PPI) foam, with the 20 and 40 PPI foams both showing a statistically significant reduction in photodegradation, which is attributed to the smaller pores blocking and reflecting more light. Small pores form a more compact structure, thereby enhancing this reflection and reducing photon interaction with the dye, preventing MB degradation. The photolytic degradation of MB was not significantly different between the control and the 5 and 10 PPI foam samples.

The MB experiments where then repeated using foams coated with TiO_2, along with TiO_2 applied as a suspension, as a fixed film, and a control sample with no foam or

catalyst. The relative loss of dye throughout the experiment is shown in Figure 4. Since each catalyst configuration contained a different amount of TiO_2, the trends in configuration effectiveness can be more clearly assessed by normalizing the MB degradation per gram of TiO_2 applied to each sample, as seen in Figure 5. Normalizing analyte degradation in this way essentially expresses the loss of MB in terms of the difference in surface area between these materials and is not intended to imply a direct or proportional increase in treatment with increasing mass of catalyst. Before and after normalizing by mass, the most effective MB degradation was observed for the suspension, with essentially complete removal of all MB by 160 minutes of exposure time. Of the remaining catalyst configurations, the fixed film, 5 PPI, 10 PPI, and 20 PPI configurations all showed similar MB removals, while the 40 PPI foam was clearly the least effective. The control sample showed ~40% dye removal over the 160 minute sampling period, consistent with degradation shown in the experiment with uncoated foams. After normalizing for TiO_2 mass, it becomes clear that the 5 and 10 PPI foams were the top performers among the immobilized configurations tested, able to achieve removals within approximately 10% of those seen with the suspension per g TiO_2. The fixed film and 20 PPI foam were intermediate performers, and the 40 PPI was the least effective configuration.

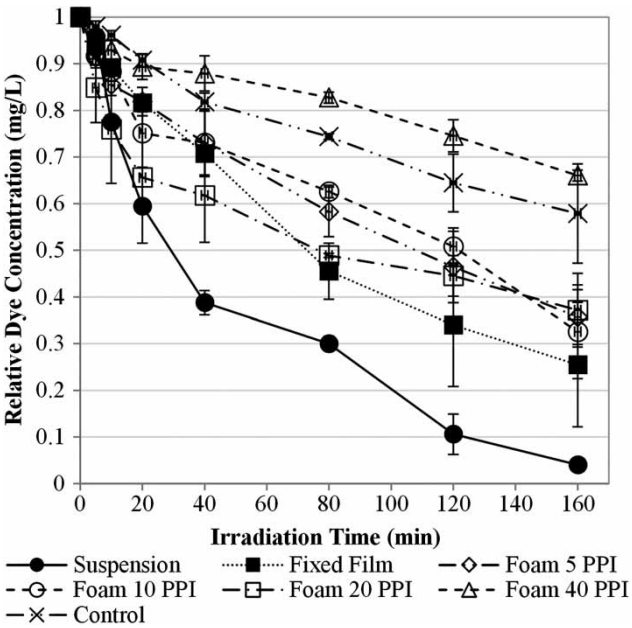

Figure 4 | Relative loss of MB for TiO_2-containing suspension, fixed film and foams of 5, 10, 20 and 40 PPI.

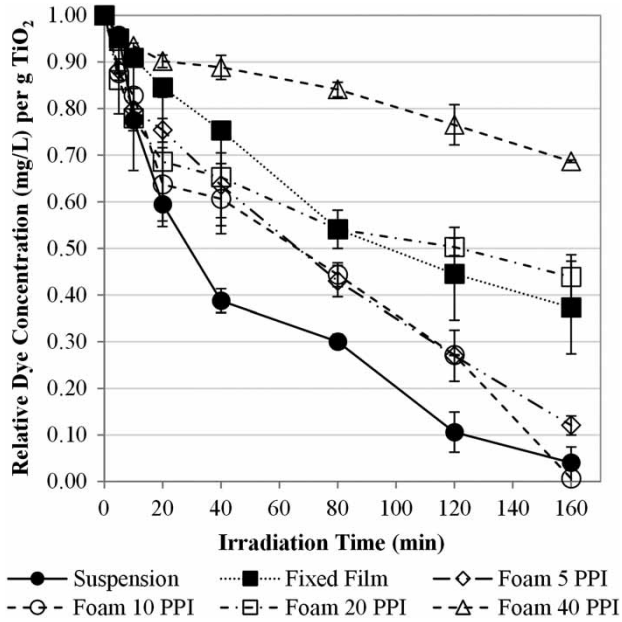

Figure 5 | Relative loss of MB for TiO_2-containing suspension, fixed film and foams of 5, 10, 20 and 40 PPI.

1,4-dioxane is a recalcitrant organic and is known to be resistant to traditional methods of decomposition, but has been shown to be effectively treated using advanced oxidation processes. This makes it an excellent candidate for characterizing the performance of the TiO_2 treatment systems in this study. As anticipated, the control sample did not show any degradation of 1,4-dioxane over a 160 minute time period in the absence of TiO_2. Figure 6 indicates that the suspension is by far the most effective, being the only configuration able to completely degrade the contaminant within 160 minutes. The data prior to normalizing for mass also show the fixed film sample was the least effective catalyst configuration, able to remove just over 20% of the 1,4-dioxane in the water sample in 160 minutes, and the foam samples were intermediate performers, able to remove between 40 and 60% of the contaminant. Normalizing by mass shows the same trends, but exaggerated, with the 5 and 10 PPI foams as the most effective configurations. Degradation efficiency decreased as the number of PPI increased beyond 10 PPI, which is attributed to the reduced amount of light entering the foam material as the pores become smaller, as shown in

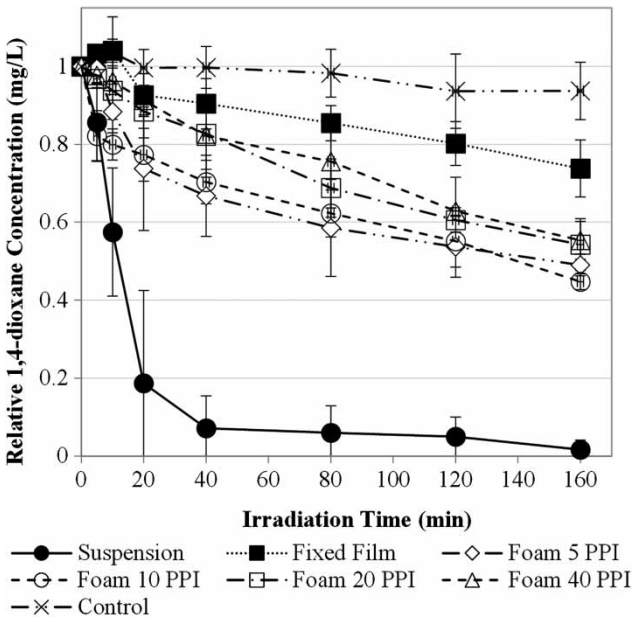

Figure 6 | Relative loss of 1,4-dioxane.

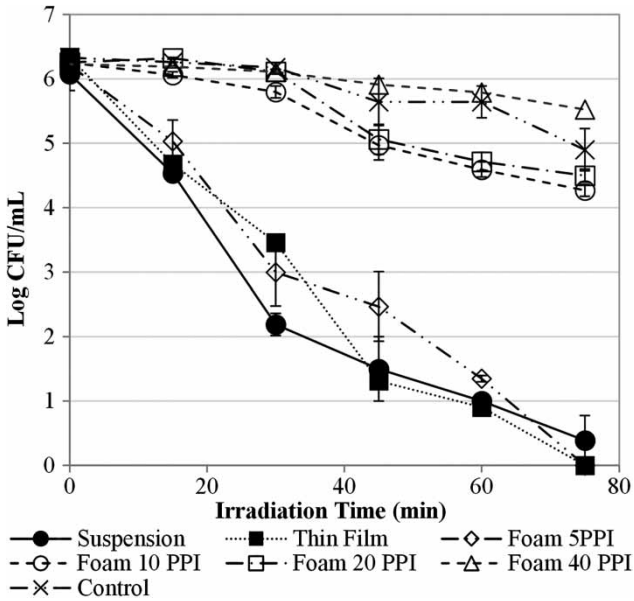

Figure 8 | Log-removal of *E. coli*.

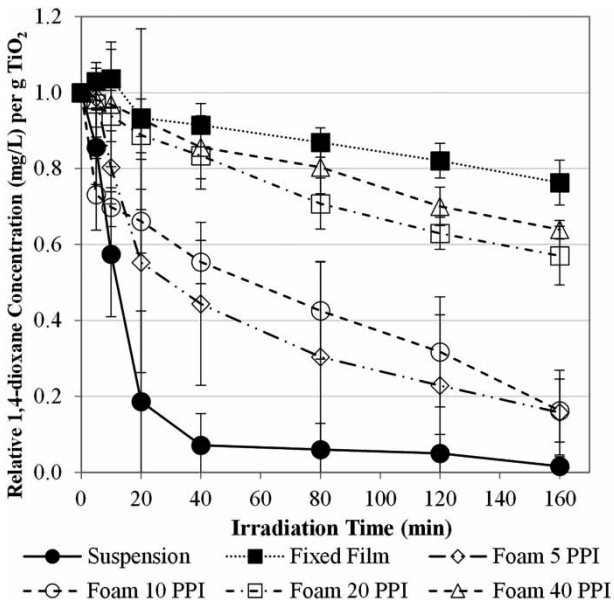

Figure 7 | Relative loss of 1,4-dioxane per g of TiO_2.

Figure 7. Photocatalytic materials are known to enhance the traditional SODIS mechanism for inactivation of *E. coli*, therefore it was anticipated that the light exposed control sample would show some inactivation, and that the samples containing photocatalytic TiO_2 would show faster and/or more complete inactivation. As shown in Figure 8, most of the TiO_2-coated foams yielded greater *E. coli* inactivation than traditional SODIS (control sample), with the 5 PPI foam in particular requiring only about 38 minutes to achieve a 3-log reduction, compared to traditional SODIS methods, which would take ~6 hours. In this practical representation of the data, prior to normalizing for mass, we see that pore densities of 10 PPI and greater have a substantial detrimental effect on the overall reactor performance.

The *E. coli* results were also normalized per gram of TiO_2, as shown in Figure 9, reaffirming that the 5 PPI foam was the most effective configuration, followed by the suspension and fixed film configurations. By determining pseudo-first order rate constants ($-k_{exp}$) after normalizing for catalyst mass, the 5 PPI foam was found to have the fastest inactivation rate. The 10 PPI and smaller pore-sized foams were less effective, with the 40 PPI foam exhibiting almost no inactivation. *E. coli* reduction therefore demonstrated a greater sensitivity to foam pore size than MB and 1,4-dioxane, where the 40 PPI foam maintained some degree of effectiveness. This could be because the *E. coli* may be less mobile than the smaller contaminants, potentially becoming associated with the foam structure. A large proportion of the bacteria might therefore remain shielded from the light, especially as the foam pore sizes become smaller.

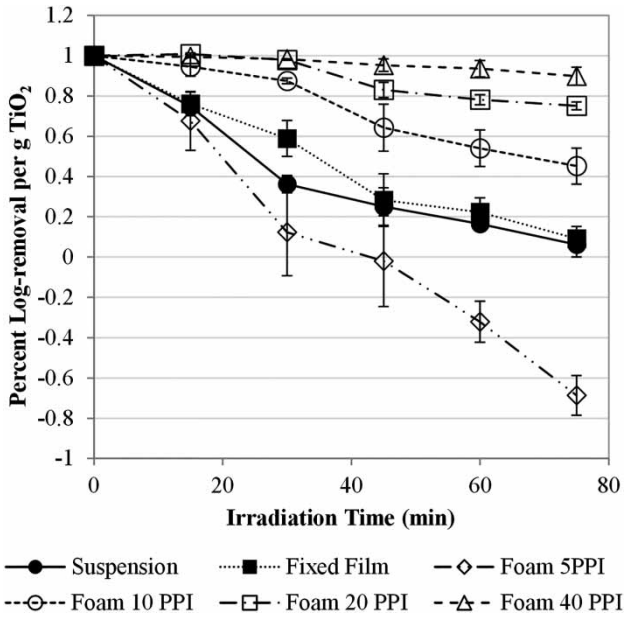

Figure 9 | Log-removal of *E. coli* per g of TiO_2.

It is also interesting to note that after normalizing for mass the 5 PPI foam achieved a higher reduction of *E. coli* than the suspension. It is proposed that the *E. coli* might attach to the foam structure more efficiently than to a TiO_2 suspension, coming into better contact with the TiO_2 and therefore experiencing a greater level of inactivation during irradiation. This would suggest that foam pore size might affect two key parameters: the ability of the light to penetrate deep into the water sample, which is impaired by pore sizes that are small, such as 40 PPI in this study, and the ability to serve as attachment locations, with the 5 PPI foam being superior to a suspension in the case of treatment for *E. coli*.

CONCLUSIONS

This study investigated the comparative performance of a SODIS-like reactor with a TiO_2 suspension to five configurations of immobilized TiO_2 with three different contaminants in a photocatalytic batch reactor under simulated solar radiation. For MB, both before and after normalizing for mass of catalyst, reactors with the 5 and 10 PPI foams were among the top performers, with performance deteriorating with the 20 and 40 PPI foams. For 1,4-dioxane, the suspension, 5 PPI and 10 PPI foam were most effective. For *E. coli*, the 5 PPI foam resulted in maximum inactivation, showing greater inactivation after 80 minutes when compared to the TiO_2 suspension and showing the fastest degradation kinetics expressed as per gram of TiO_2. The 40 PPI foam was a poor performer for all contaminants. It is presumed that the very fine pore size of the foam prevented light from radiating through the water sample. This is supported by the decrease in photolytic degradation of MB observed in the control experiment. Overall, it was observed that TiO_2 catalyst immobilized on a foam support could match the efficiency of a suspension. Performance was related to foam pore size and an optimum pore size of 5–10 PPI was observed; however, the optimum conditions were a function of the target contaminant. *E. coli* appeared to be the most sensitive to pore size, possibly due to lower mobility during exposure to light than the chemical contaminants. The results of this work are intended to guide future research into methods to improve SODIS effectiveness by using immobilized TiO_2 on a foam support. The results suggest that a foam support with a pore size in the range of 5–10 PPI may provide significant treatment performance relative to a SODIS system that is free of the photocatalyst, while allowing the photocatalyst to be easily removed following treatment and potentially reused.

ACKNOWLEDGEMENTS

Funding for the work was generously provided by the Natural Sciences and Engineering Research Council Chair in Drinking Water Research, the Southern Ontario Water Consortium, and the Ontario Graduate Scholarship program.

REFERENCES

Acra, A., Jurdi, M., Allem, H. M, Karahagopian, Y. & Raffoul, Z. 1990 *Water Disinfection by Solar Radiation: Assessment and Application*. Report No. 0140–6736, International Development Research Centre, Ottawa, ON, Canada.

Akhavan, O., Abdolahad, M., Abdi, Y. & Mohajerzadeh, S. 2009 Synthesis of titania/carbon nanotube heterojunction arrays for photoinactivation of *E. coli* in visible light irradiation. *Carbon* **47**, 3280–3287.

Antoniou, M. G., Nicolaou, P. A., Shoemaker, J. A., de la Cruz, A. A. & Dionysiou, D. D. 2009 Impact of the morphological

properties of thin TiO_2 photocatalytic films on the detoxification of water contaminated with the cyanotoxin, microcystin-LR. *Appl Catal. B-Environ.* **91**, 165–173.

Blanco, J., Malato, S., Fernandez-Ibanez, P., Alarcon, D., Gernjak, W. & Maldonado, M. L. 2009 Review of feasible solar energy applications to water processes. *Renew. Sust. Energ. Rev.* **13**, 1437–1445.

Byrne, J. A., Fernandez-Ibanez, P. A., Dunlop, P. S. M., Alrousan, D. M. A. & Hamilton, J. W. J. 2011 Photocatalytic enhancement for solar disinfection of water: a review. *Intl J. Photoenergy* **2011**, 1–12.

Cho, M., Chung, H., Choi, W. & Yoon, J. 2004 Linear correlation between inactivation of *E-coli* and OH radical concentration in TiO_2 photocatalytic disinfection. *Water Res.* **38**, 1069–1077.

Galalgorchev, H. 1992 WHO guidelines for drinking-water quality. *Water Supp.* **11**, 1–16.

Guiang, L., Jun, Z., Xuemin, H. & Chenwen, X. Research on photocatalytic activity of Nano-TiO2 coating on foam Al by composite electroplating. IEEE 307–309.

Gumy, D., Rincon, A. G., Hajdu, R. & Pulgarin, C. 2006 Solar photocatalysis for detoxification and disinfection of water: different types of suspended and fixed TiO_2 catalysts study. *Sol. Energy* **80**, 1376–1381.

Han, C., Pelaez, M., Likodimos, V., Kontos, A. G., Falaras, P., O'Shea, K. & Dionysiou, D. D. 2011 Innovative visible light-activated sulfur doped TiO_2 films for water treatment. *Appl. Catal. B-Environ.* **107**, 77–87.

Kisch, H. & Macyk, W. 2002 Visible-light photocatalysis by modified titania. *Chemphyschem.* **3**, 399–400.

Li, Q., Page, M. A., Marinas, B. J. & Shang, J. K. 2008 Treatment of coliphage MS2 with palladium-modified nitrogen-doped titanium oxide photocatalyst illuminated by visible light. *Environ. Sci. Technol.* **42**, 6148–6153.

Lonnen, J., Kilvington, S., Kehoe, S. C., Al-Touati, F. & McGuigan, K. G. 2005 Solar and photocatalytic disinfection of protozoan, fungal and bacterial microbes in drinking water. *Water Res.* **39**, 877–883.

Luck, A. & Hofmann, R. 2006 UV/TiO_2 for Drinking Water Treatment: Concurrent Degradation of 1, 4-Dioxane and Removal of Iron and Manganese. Master's Thesis, Department of Civil Engineering, University of Toronto, Canada.

Meierhofer, R. & Wegelin, M. 2002 *Solar Water Disinfection: A Guide for the Application of SODIS*. Report No. No 06/02; SANDEC (Water & Sanitation in Developing Countries) at EAWAG (Swiss Federal Institute for Environmental Science and Technology), Duebendorf, Switzerland.

Natarajan, K., Natarajan, T. S., Bajaj, H. C. & Tayade, R. J. 2011 Photocatalytic reactor based on UV-LED/TiO_2 coated quartz tube for degradation of dyes. *Chem Eng. J.* **178**, 40–49.

Plantard, G., Goetz, V., Correia, F. & Cambon, J. P. 2011 Importance of a medium's structure on photocatalysis: using TiO_2-coated foams. *Sol. Energ. Mat. Sol. C* **95**, 2437–2442.

Plesch, G., Gorbar, M., Vogt, U. F., Jesenak, K. & Vargova, M. 2009 Reticulated macroporous ceramic foam supported TiO_2 for photocatalytic applications. *Mater Lett.* **63**, 461–463.

Sahoo, C. & Gupta, A. K. 2012 Optimization of photocatalytic degradation of methyl blue using silver ion doped titanium dioxide by combination of experimental design and response surface approach. *J. Hazard Mater.* **215**, 302–310.

Shannon, M. A., Bohn, P. W., Elimelech, M., Georgiadis, J. G., Marinas, B. J. & Mayes, A. M. 2008 Science and technology for water purification in the coming decades. *Nature* **452**, 301–310.

Wang, W. Y. & Ku, Y. 2006 Photocatalytic degradation of Reactive Red 22 in aqueous solution by UV-LED radiation. *Water Res.* **40**, 2249–2258.

Zhang, D. F. 2012 Photocatalytic applications of Au-deposited on TiO_2 nanocomposite catalyst in dye degradation via photoreduction. *Russ. J. Phys. Chem. A* **86**, 498–503.

Zhang, Z. H., Wu, H. J., Yuan, Y., Fang, Y. J. & Jin, L. T. 2012 Development of a novel capillary array photocatalytic reactor and application for degradation of azo dye. *Chem. Eng. J.* **184**, 9–15.

First received 6 March 2015; accepted in revised form 11 June 2015. Available online 10 July 2015